Stability of flows induced by a surface acoustic wave along a slab

2003 J. Phys. A: Math. Gen. 36 5817

(http://iopscience.iop.org/0305-4470/36/21/310)

INSTITUTE OF PHYSICS PUBLISHING JOURNAL OF PHYSICS A: MATHEMATICAL AND GENERAL

J. Phys. A: Math. Gen. **36** (2003) 5817–5824 PII: S0305-4470(03)58259-2

Stability of flows induced by a surface acoustic wave along a slab

Kwang-Hua W Chu

Department of Physics, Northwest Normal University, Gansu, Lanzhou 730070, People's Republic of China

Received 6 January 2003, in final form 9 April 2003
Published 13 May 2003
Online at stacks.iop.org/JPhysA/36/5817

Abstract

The stability of flows of Newtonian fluids induced by a surface acoustic wave (SAW) along the deformable walls in a confined parallel-plane microchannel or slab in the laminar flow regime is investigated. The governing equation which was derived by considering the weakly nonlinear coupling between the deformable wall and viscous flow is linearized and then the eigenvalue problem is solved by a numerical code together with the associated interface and boundary conditions. The value of the critical Reynolds number was found to be near 613.26 which is much smaller than the static-wall case: 5772 for conventional pressure-driven flows.

PACS numbers: 47.20.Ma, 02.30.Mv, 43.35.Pt, 68.08.−p, 47.62.+q, 43.38.Rh, 43.25.Nm

1. Introduction

The application of linear and/or nonlinear surface acoustic waves (SAW, say, nondispersive Rayleigh waves and dispersive perturbed Rayleigh waves [1]) and their relevant studies have been reported in diverse fields such as condensed matter physics, materials science or surface chemistry/physics, environmental, communication and sensor technologies, etc [1–3]. Fundamental or theoretical (using the Boltzmann equation) and experimental studies of interphase nonlocal transport phenomena in a gas–solid system which appear due to the propagation of a surface acoustic wave (SAW) in a solid-wall had been performed since late 1980s [4–6]. Preliminary theoretical results in a free molecular regime showed some disagreement with other approaches [4–6].

Meanwhile, the emerging interest in current applications of MEMS (Microelectromechanical system) [7, 8] and especially microfluidics [9–11] which require handling fluids has stimulated some new areas of research: development of new methods for fabricating fluidic systems, invention of flexible components from which to assemble functionally complex fluidic devices and examination of the fundamental behaviour

of fluids in microchannels [12, 13]. The challenges are how to overcome or control macroscopically ambient or environmental noises which are of significance in microdomains [14]. Considering the soft or flexible organic ICs [15–17], which are not so rigid as the traditional one (e.g. metals or alloys) and the typical micron-thickness of the wall (even the material is silicon-based), we shall take into account the nonsteady effect due to non-static noise upon the walls as the fluid is flowing within these rather thin or soft walls [15–17].

Recently researchers have started to investigate the transport within a soft or deformable microslab which will be common in microdomains of bio-MEMS applications and found interesting physical behaviours due to the weakly nonlinear coupling between the surface wave and the slip velocity along the wall [18–23].

To further study the stability issues for laminar flows of Newtonian fluids in microdomains, we solve the eigenvalue problem by a numerical code based on the spectral method for obtaining the neutral boundary curves. The flow is induced by a sinusoidal wave travelling down the walls of a 2D microchannel of constant width and rather long length or a microslab [19, 20, 22, 23].

We first adopt the continuum-mechanics approach and simplify the original system of equations (related to the momentum and mass transport) to one single higher order quasi-linear partial differential equation in terms of the unknown stream function. In this study, we shall assume that the Mach number Ma $\ll$ 1, and the governing equations are the incompressible Navier–Stokes equations which are solved together with the no-slip boundary conditions along the walls [19, 20, 22, 23]. Note that if the thickness of the flexible wall is smaller than the wavelength of SAW then the SAW is dispersive. We introduce the perturbation technique so that we can obtain the related governing equations and then solve the relevant eigenvalue problem approximately. That is to say, after linearizing the originally derived nonlinear partial differential equation, we then solve a fourth-order quasi-linear complex ordinary differential equation together with the wavy boundary or interface conditions by verified numerical methods [24–26, 28]. We can finally get the critical Reynolds number corresponding to the specific wave number after intensive calculations.

2. Formulations

2.1. Derivation of the governing equation and boundary conditions

We consider a 2D channel of uniform thickness filled with a homogeneous Newtonian fluid. The flat-plane walls of the channel are rather flexible, on which are imposed travelling sinusoidal waves of small amplitude a (due to SAW). The vertical displacements of the upper and lower walls ($y = d$ and $y = -d$) are thus assumed to be η and $-\eta$, respectively, where $\eta = a\cos\frac{2\pi}{\lambda}(x - ct)$, λ is the wavelength and c the SAW speed. x and y are Cartesian coordinates, with x measured in the direction of wave propagation and y measured in the direction normal to the mean position of walls. We note that, if the thickness of the flexible wall is presumed to be not smaller than the wavelength of SAW, we then consider the treatment of nondispersive SAWs in homogeneous media (cf page 43 or 45 of [1]). The schematic plot of above features is shown in figure 1.

For the easy treatment of tedious mathematical manipulations we simplify equations by introducing dimensionless variables. We have a characteristic velocity c and three characteristic lengths a, λ and d. The following variables based on c and d are thus

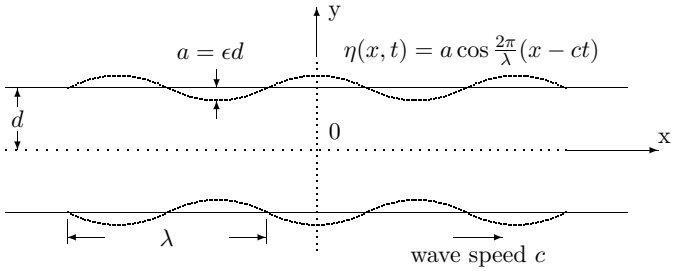

Figure 1. Schematic diagram of the wavy motion of the flexible walls.

introduced:

$$x' = \frac{x}{d} \qquad y' = \frac{y}{d} \qquad u' = \frac{u}{c} \qquad v' = \frac{v}{c}$$
$$\eta' = \frac{\eta}{d} \qquad \psi' = \frac{\psi}{cd} \qquad t' = \frac{ct}{d} \qquad p' = \frac{p}{\rho c^2}$$

where ψ is the dimensional stream function. The amplitude ratio ϵ, the dimensionless wave number α, and the Reynolds number Re are defined by

$$\epsilon = \frac{a}{d} \qquad \alpha = \frac{2\pi d}{\lambda} \qquad \mathrm{Re}_c = \frac{cd}{\nu}.$$

From now on, we drop the prime in our notation for the dimensionless variables. We shall seek a solution in the form of a series in the parameter ϵ:

$$\psi = \psi_0 + \epsilon\psi_1 + \epsilon^2\psi_2 + \cdots \qquad \frac{\partial p}{\partial x} = \left(\frac{\partial p}{\partial x}\right)_0 + \epsilon\left(\frac{\partial p}{\partial x}\right)_1 + \epsilon^2\left(\frac{\partial p}{\partial x}\right)_2 + \cdots$$

with the velocity $\mathbf{v} = (u, v)$, where $u = \partial\psi/\partial y$, $v = -\partial\psi/\partial x$. The 2D ($x$- and y-) momentum equations

$$\frac{\partial \mathbf{v}}{\partial t} + \mathbf{v}\cdot\nabla\mathbf{v} = -\nabla p + \frac{\nabla^2\mathbf{v}}{\mathrm{Re}_c}$$

and the equation of continuity: $\nabla\cdot\mathbf{v} = 0$ are written in terms of the stream function ψ only by eliminating the pressure (p) term. The final governing equation is

$$\frac{\partial}{\partial t}\nabla^2\psi + \psi_y\nabla^2\psi_x - \psi_x\nabla^2\psi_y = \frac{1}{\mathrm{Re}_c}\nabla^4\psi \qquad \nabla^2 \equiv \frac{\partial^2}{\partial x^2} + \frac{\partial^2}{\partial y^2} \tag{1}$$

and subscripts indicate the partial differentiation. Thus, we have

$$\frac{\partial}{\partial t}\nabla^2\psi_0 + \psi_{0y}\nabla^2\psi_{0x} - \psi_{0x}\nabla^2\psi_{0y} = \frac{1}{\mathrm{Re}_c}\nabla^4\psi_0 \tag{2}$$

$$\frac{\partial}{\partial t}\nabla^2\psi_1 + \psi_{0y}\nabla^2\psi_{1x} + \psi_{1y}\nabla^2\psi_{0x} - \psi_{0x}\nabla^2\psi_{1y} - \psi_{1x}\nabla^2\psi_{0y} = \frac{1}{\mathrm{Re}_c}\nabla^4\psi_1 \tag{3}$$

$$\frac{\partial}{\partial t}\nabla^2\psi_2 + \psi_{0y}\nabla^2\psi_{2x} + \psi_{1y}\nabla^2\psi_{1x} + \psi_{2y}\nabla^2\psi_{0x} - \psi_{0x}\nabla^2\psi_{2y}$$
$$- \psi_{1x}\nabla^2\psi_{1y} - \psi_{2x}\nabla^2\psi_{0y} = \frac{1}{\mathrm{Re}_c}\nabla^4\psi_2 \tag{4}$$

and other higher order terms. The gas is subjected to boundary conditions imposed by the symmetric motion of the walls and the no-slip condition: $u = 0$, $v = \pm\partial\eta/\partial t$ at $y = \pm(1+\eta)$.

The boundary conditions may be expanded in powers of η and then ϵ:

$$\begin{aligned}
&\psi_{0y}|_1 + \epsilon\{\cos\alpha(x-t)\psi_{0yy}|_1 + \psi_{1y}|_1\} \\
&\qquad + \epsilon^2\left\{\frac{\psi_{0yyy}|_1}{2}\cos^2\alpha(x-t) + \psi_{2y}|_1 + \cos\alpha(x-t)\psi_{1yy}|_1\right\} + \cdots = 0 \\
&\psi_{0x}|_1 + \epsilon\{\cos\alpha(x-t)\psi_{0xy}|_1 + \psi_{1x}|_1\} + \epsilon^2\left\{\frac{\psi_{0xyy}|_1}{2}\cos^2\alpha(x-t)\right. \\
&\qquad \left. + \cos\alpha(x-t)\psi_{1xy}|_1 + \psi_{2x}|_1\right\} + \cdots = -\epsilon\alpha\sin\alpha(x-t).
\end{aligned} \tag{5}$$

Equations (2) and (5) above, together with the condition of symmetry (for u-velocity profile) and a uniform constant pressure-gradient in the x-direction for the flow of order 0 (if $(\partial p/\partial x)_0 = 0$, then the gas is originally quiescent; this corresponds to a free pumping case [18–20, 22, 23]), yield:

$$\psi_0 = K_0\left[y - \frac{y^3}{3}\right] = 0 \qquad K_0 = \frac{\mathrm{Re}_c}{2}\left(-\frac{\partial p}{\partial x}\right)_0 \tag{6}$$

which is, in fact, a plane Poiseuille flow;

$$\psi_1 = \tfrac{1}{2}\{\phi(y)\,\mathrm{e}^{\mathrm{i}\alpha(x-t)} + \phi^*(y)\,\mathrm{e}^{-\mathrm{i}\alpha(x-t)}\} \tag{7}$$

where the asterisk denotes the complex conjugate. A substitution of ψ_1 into equation (3) yields

$$\left\{\frac{\mathrm{d}^2}{\mathrm{d}y^2} - \alpha^2 + \mathrm{i}\alpha\,\mathrm{Re}_c[1 - K_0(1-y^2)]\right\}\left(\frac{\mathrm{d}^2}{\mathrm{d}y^2} - \alpha^2\right)\phi - 2\mathrm{i}\alpha K_0\,\mathrm{Re}_c\phi = 0. \tag{8}$$

The associated boundary conditions are

$$\phi_y(\pm 1) = 2K_0 \qquad \phi(\pm 1) = \pm 1. \tag{9}$$

Note that, once we set $K_0 = 0$, we then obtain

$$\left(\frac{\mathrm{d}^2}{\mathrm{d}y^2} - \alpha^2\right)\left(\frac{\mathrm{d}^2}{\mathrm{d}y^2} - \bar{\alpha}^2\right)\phi = 0 \qquad \bar{\alpha}^2 = \alpha^2 - \mathrm{i}\alpha\,\mathrm{Re}_c.$$

After lengthy algebraic manipulations, we obtain

$$\phi = c_0\,\mathrm{e}^{\alpha y} + c_1\,\mathrm{e}^{-\alpha y} + c_2\,\mathrm{e}^{\bar{\alpha} y} + c_3\,\mathrm{e}^{-\bar{\alpha} y}$$

where $c_0 = (A + A_0)/\mathrm{det}$, $c_1 = -(B + B_0)/\mathrm{det}$, $c_2 = (C + C_0)/\mathrm{det}$, $c_3 = -(T + T_0)/\mathrm{det}$;

$$\mathrm{det} = Ae^{\alpha} - Be^{-\alpha} + Ce^{\bar{\alpha}} - Te^{-\bar{\alpha}}$$

(see [18, 22] for the details).

These terms and the determination of ψ_2 are useful for the calculation of the mean flux (averaged over one wavelength of the SAW) which has been reported in [18, 23] for cases of $K_0 = 0$ (free pumping) but not relevant to present stability problems.

2.2. Numerical approaches

To obtain the stability characteristics for SAW-driven flows by using verified codes developed before [24, 25] for calculating the Orr–Sommerfeld spectra, we transform equation (8) into the Orr–Sommerfeld form by rescaling and redimensionalization of physical parameters and variables mentioned before (e.g., the careful selection of K_0 and c).

Note that, the plane Poiseuille flow is one of the fundamental base-flow types for the wall-bounded parallel-flow-instability research regime. If considering the linear stability of

the laminar flow, the usual approach is through the Orr–Sommerfeld (OS) equation [24–27]. Following the usual assumptions of linearized stability theory [24–27], we have $v_i(x_i, t) = \bar{v}_i(x_i) + v_i'(x_i, t)$, and similarly, $p(x_i, t) = \bar{p}(x_i) + p'(x_i, t)$ for the velocity and pressure terms in the incompressible Navier–Stokes equations [27]. Then by substituting these into dimensionless 2D Navier–Stokes equation, and eliminating the pressure terms, the linearized equation (in terms of the stream function of the disturbance) or the so-called Orr–Sommerfeld equation [26, 27], which governs the variation of the disturbances is

$$(D^2 - \alpha^2)^2\phi = \mathrm{i}\alpha\,\mathrm{Re}[(\bar{u} - \sigma)(D^2 - \alpha^2)\phi - (D^2\bar{u})\phi] \tag{10}$$

where $D = \mathrm{d}/\mathrm{d}y$, $\mathrm{Re} = \rho u_{\max} d/\mu$ is the Reynolds number based on half channel-width (d), $u_{\max}$ is the maximum velocity across the channel-width; $\bar{u} = 1 - y^2$ is the (mean) basic velocity profile of the flow for $-1 \leqslant y \leqslant 1$. σ is a complex value or the eigenvalue we like to obtain. The stream function for the disturbance, Ψ, such that $u' = -\partial\Psi/\partial y$, $v' = -\partial\Psi/\partial x$, were assumed to have the form $\Psi(x, y, t) = \phi(y)\exp[\mathrm{i}\alpha(x - \sigma t)]$ in the usual normal-mode analysis, α is wave number (real) and σ is $\sigma_r + \mathrm{i}\sigma_i$. This is a kind of Tollmien–Schlichting transversal waves, σ_r is the ratio between the velocity of propagation of the wave of perturbation and the characteristic velocity, σ_i is called the amplification factor and α equals $2\pi L^{-1}$, where L is the wavelength of the Tollmien–Schlichting perturbation [27].

Boundary and interface conditions for ϕ or $D\phi$ are already defined in equation (9) and are not the same as previous approaches [24–26], i.e., $\phi(\pm 1) = D\phi(\pm 1) = 0$.

The eigenvalue problem raised above could then be solved by using the verified code [24, 25], which followed and adopted the spectral method [28] based on the Chebyshev-polynomial-expansion approach, after the equation and boundary conditions are discretized. The algebraic equation is

$$\begin{aligned}
\frac{1}{24} \sum_{\substack{p=n+4 \\ p\equiv n(\mathrm{mod}\,2)}}^{N} & [p^3(p^2-4)^2 - 3n^2p^5 + 3n^4p^5 + 3n^4p^3 - pn^2(n^2-4)^2]a_p \\
& - \sum_{\substack{p=n+2 \\ p\equiv n(\mathrm{mod}\,2)}}^{N} \left\{ \left[2\alpha^2 + \frac{1}{4}\mathrm{i}\alpha\,\mathrm{Re}(4f - 4\sigma - c_n - c_{n-1}) \right] p(p^2 - n^2) \right. \\
& \left. - \frac{1}{4}\mathrm{i}\alpha\,\mathrm{Re}\,c_n\,p[p^2 - (n+2)^2] - \frac{1}{4}\mathrm{i}\alpha\,\mathrm{Re}\,d_{n-2}\,p[p^2 - (n-2)^2] \right\} a_p \\
& + \mathrm{i}\alpha\,\mathrm{Re}\,n(n-1)a_n + \{\alpha^4 + \mathrm{i}\alpha\,\mathrm{Re}[(f - \sigma)\alpha^2 - 2]\}c_n a_n \\
& - \frac{1}{4}\mathrm{i}\alpha^3\,\mathrm{Re}[c_{n-2}a_{n-2} + c_n(c_n + c_{n-1})a_n + c_n a_{n+2}] = 0
\end{aligned} \tag{11}$$

for $n \geqslant 0$, $f = 1$, where $c_n = 0$ if $n > 0$, and $d_n = 0$ if $n < 0$, $d_n = 1$ if $n \geqslant 0$. Here, $\sigma \equiv C$ is the complex eigenvalue, N is the number of maximum expansion terms $\left(\phi = \sum_n^N a_n T_n\right)$ for the Chebyshev polynomial: T_n, n is the corresponding index for T_n [24–26, 28]. c_n and d_n are the control constants. The boundary conditions become

$$\sum_{\substack{n=0 \\ n\equiv 0(\mathrm{mod}\,2)}}^{N} a_n = 1 \qquad \sum_{\substack{n=0 \\ n\equiv 0(\mathrm{mod}\,2)}}^{N} n^2 a_n = 2K_0 \tag{12}$$

$$\sum_{\substack{n=1 \\ n\equiv 1(\mathrm{mod}\,2)}}^{N} a_n = -1 \qquad \sum_{\substack{n=1 \\ n\equiv 1(\mathrm{mod}\,2)}}^{N} n^2 a_n = 2K_0. \tag{13}$$

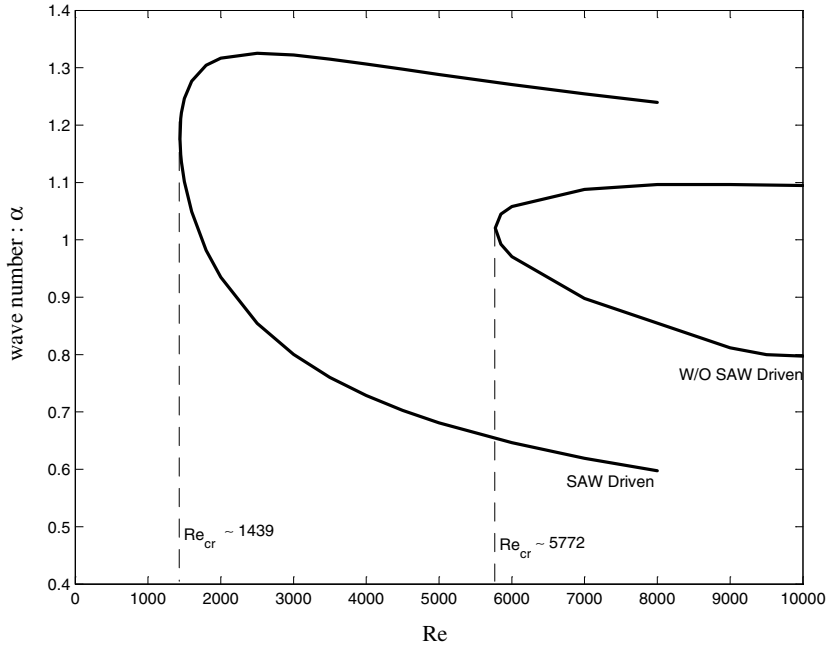

Figure 2. SAW effects ($K_0 = 1$) on the neutral stability boundary of the plane Poiseuille flow. Re_{cr} is the critical Reynolds number of the flow. For SAW-driven case, $\mathrm{Re}_{cr} \sim 1439$.

The matrices thus formed are not diagonally dominated and symmetric [24, 25, 29]. Before we perform floating-point computations to get the complex eigenvalues, we should precondition these complex matrices to get less errors. Here we adapt Osborne's algorithm [29] to precondition these complex matrices by diagonal similarity transformations of the matrix (errors are in terms of the Euclidean norm of the matrix) designed to reduce its norm [24, 25]. The details of this algorithm could be traced in [24, 25]. The form of the reduced matrix is upper Hessenberg. We then perform the stabilized LR transformations for these matrices to get the eigenvalues σ or $C = C_r + \mathrm{i}\, C_i$ (please see also [24, 25] for the details).

3. Results and discussion

The preliminary verified results of this numerical code had been reported [24, 25] for the cases of no-slip boundary conditions (plane Poiseuille flows without SAW propagating along the walls) in comparison with the benchmark results of Orszag's [26]. For example, for $\mathrm{Re} = 10000.0$, $\alpha = 1.0$ of the test case: plane Poiseuille flow [26], we obtained the same spectrum as 0.23752648 + i 0.00373967 for $C_r + \mathrm{i}\, C_i$ [24, 25] which Orszag obtained from CDC 7600 using the spectral method in 1971 [26].

We subsequently calculated those spectra for the SAW-driven flow with the associated dynamic and/or kinematic boundary (interface) conditions by carefully adjusting the Reynolds number (Re) and the wave number (α). After intensive calculations, we finally obtain the neutral boundary curves for specific Re and α and plot them in figure 2. K_0 was fixed as one here. For comparison with the neutral stability curve obtained for flows without SAW-driven mechanism (there is no SAW propagating along the walls), we put both curves in one figure. Note that each curve is composed of two branches (one is upper and the other

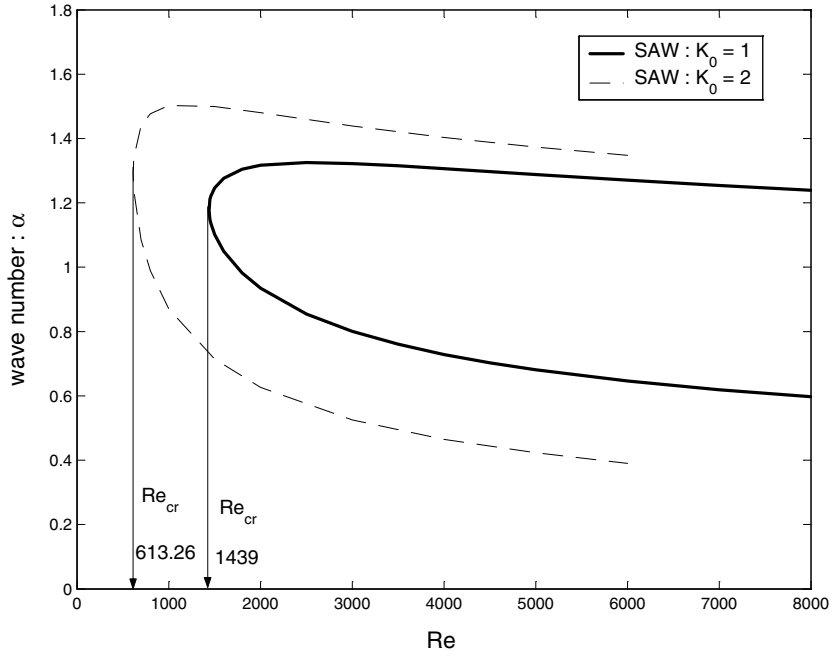

Figure 3. SAW effects ($K_0 = 1$ and 2) on the neutral stability boundary of the plane Poiseuille flow. Re_{cr} is the critical Reynolds number of the flow. For $K_0 = 2$ case, $\mathrm{Re}_{cr} \sim 613.26$ (dashed curve).

is lower, they coalesce into a critical point (Re_{cr} and α_{cr})). For those flows with Re and α falling within these branches or the boundary, perturbations amplify temporarily [25–27] and thus they are unstable. That is to say, any small disturbances will amplify in a finite time and/or in the downstream when Re and α are larger than the critical ones (Re_{cr} w.r.t. the specific α_{cr}) which are fixed upon the curves. We have roughly $\mathrm{Re}_{cr} = 1439$ for SAW-driven flows when $K_0 = 1$. The critical Reynolds number for conventional flows (without SAW propagating along the walls) is around 5772 [26]. To further illustrate the SAW effects, we plot cases of $K_0 = 1$ and $K_0 = 2$ in figure 3. As K_0 increases, Re_{cr} decreases and becomes 613.26.

In brief conclusion, we can observe that SAW triggers the instability of the laminar flow much earlier ($\mathrm{Re}_{cr} \sim 613$) which is not favourable for the flow control in some applications of MEMS or bio-MEMS, such as drag-reduction of micro air vehicles [30] or DNA manipulations in ambient fluids (in contrast, it will be useful for micro-flow mixing or osmosis). Our observation might be interpreted as due to the coupling between the flexible wall-boundary and the inertia of the acoustic-streaming flow. We hope that in the future we can investigate other issues of diverse SAW applications [31–33] using the present or more advanced approach.

Acknowledgments

This project is supported by the National Natural Science Foundation of China (NNSFC) under grant no 10274061. The author would like to thank the referees for their stimulating comments.

References

[1] Hess P 2002 *Phys. Today* **55** 42
[2] Assouar M B *et al* 2000 *Appl. Surf. Sci.* **164** 200
[3] Ploetner M *et al* 1999 *Transducers'99* pp 640
[4] Borman V D, Krylov Yu S and Kharitonov A M 1987 *Sov. Phys.– JETP* **65** 935
[5] Aleksandrov O E *et al* 1989 *Sov. Phys. Acoust.* **35** 561
Aleksandrov O E and Seleznev V D 1995 *J. Stat. Phys.* **78** 161
[6] Terry P and Strandberg M W P 1981 *J. Appl. Phys.* **52** 4281
[7] Bishop D, Gammel P and Giles R 2001 *Phys. Today* **54** 38
[8] Nagel D J and Zaghloul M E 2001 *IEEE Circuits Devices Mag.* **17** 14
[9] Fan Z F *et al* 2002 *J. Micromech. Microeng* **12** 655
[10] Giordano N and Cheng J-T 2001 *J. Phys.: Condens. Matter* **13** R271
[11] Urbanek W, Zemel J N and Bau H H 1993 *J. Micromech. Microeng* **3** 206
[12] Whitesides G M and Stroock A D 2001 *Phys. Today* **54** 42
[13] Heuberger M, Zäch M and Spencer N D 2001 *Science* **292** 905
[14] Esashi M, Minami K and Ono T 1998 *Cond. Matter News* **6** 31
[15] Crone B, Dodabalapur A and Lin Y Y 2000 *Nature* **403** 521
[16] Dodabalapur A, Torsi L and Katz H E 1995 *Science* **268** 270
[17] Drury C J *et al* 1998 *Appl. Phys. Lett.* **73** 108
[18] Chu K-H W 2002 *Eur. Phys. J. Appl. Phys.* **18** 51
[19] Selverov K P and Stone H A 2001 *Phys. Fluids* **13** 1837
[20] Chu K-H W 2002 *Phys. Scr.* **65** 28
[21] Kogan M N 1969 *Rarefied Gas Dynamics* (New York: Plenum)
[22] Fung Y C and Yih C S 1968 *J. Appl. Mech.* **35** 669
[23] Chu A K-H 2002 *Electron. Lett.* **38** 1481
Chu K-H W 2003 *Preprint*
[24] Chu W K-H 2000 *J. Phys.: Condens. Matter* **12** 8065
[25] Chu W K-H 2001 *J. Phys. A: Math. Gen.* **34** 3389
[26] Orszag S A 1971 *J. Fluid Mech.* **50** 689
[27] Georgescu A 1985 *Hydrodynamic Stability Theory* (translation edited by D Sattinger) (Dordrecht: Martinus Nijhoff)
[28] Gottlieb D and Orszag S A 1977 *Numerical Analysis of Spectral Methods: Theory and Aplications* (Philadelphia: SIAM) (NSF-CBMS Monograph No. 26)
[29] Osborne E E 1960 *J. Assoc. Comput. Mach.* **7** 338
[30] Zbikowski R 2001 *Phil. Trans. Math. Phys. Eng. Sci.* **360** 273
[31] Glorieux C *et al* 2000 *J. Appl. Phys.* **88** 4394
[32] Levinson Y, Entin-Wohlman O and Wolflem P 2000 *Phys. Rev. Lett.* **85** 634
[33] Barnes C H W, Shilton J M and Robinson A N 2000 *Phys. Rev.* B **62** 8410